Raman scattering from a self-organized Ge dot superlattice

J. L. Liu,[a] Y. S. Tang, and K. L. Wang
Device Research Laboratory, Department of Electrical Engineering, University of California at Los Angeles, Los Angeles, California 90095-1594

T. Radetic and R. Gronsky
Materials Science & Mineral Engineering, University of California at Berkeley, Berkeley, California 94720-1760

(Received 17 November 1998; accepted for publication 2 February 1999)

We present a Raman scattering study of a self-organized Ge dot superlattice. The structure, which consists of 20 periods of Ge quantum dots sandwiched by 6 nm Si spacers, is grown on a Si (100) substrate by solid source molecular beam epitaxy. Cross-sectional transmission electron microscopy is used to characterize the structural properties of these Ge dots. Raman spectrum shows a downward shift of the Ge–Ge mode, which is attributed to the phonon confinement in the Ge dots. From polarization dependent Raman spectra, strong inter-sub-level transition in the Ge quantum dots is observed. From a simple calculation, the observed peak at 1890 cm^{-1} in the polarized spectrum is attributed to the transition between the first two heavy hole states of the Ge quantum dots. © *1999 American Institute of Physics.* [S0003-6951(99)04213-8]

Semiconductor quantum dot structures represent the ultimate case of size quantization in semiconductors. The electronic structure of an ideal quantum dot is composed of a set of discrete energy levels where the charged carriers are confined in all three dimensions. Hence, quantum dots provide a unique way to tailor the optical and electrical properties for designing and developing a new class of photonic devices, such as lasers and detectors.[1] Recently, the formation of self-organized semiconductor quantum dots by the Stranski–Krastanow growth process has attracted much attention. The structural properties and interband optical properties of these quantum dots have been widely reported in the literature.[2–5] Inter-sub-level optical transition is an alternate subject of interest. To date, most of the work in this field is based on optical transitions of electrons within the conduction band in III–V quantum dot structures.[6–8] Little work is done on the valence band inter-sub-level spectroscopy in any quantum dot system and, in particular, in SiGe-based quantum dot structures. The fact that most of the band-gap discontinuity (between Si and Ge) goes to the valence band as well as the small hole effective mass favors hole inter-sub-level transitions for midinfrared applications. Furthermore, the polarization selection rules of inter-sub-level transitions[9] strongly depend on the spatial distribution and the symmetry of the levels involved in the transitions and therefore, can be utilized to study the characteristics of the energy levels. Recently, we have obtained the evidence for heavy-hole inter-sub-level absorption in self-organized Ge quantum dots.[10] However, more work in this field needs to be done.

Previously, Raman spectroscopy has been used to study the phonon and energy level spectrum of quantum wells.[11–13] Compared with scattering processes in quantum wells, inter-sub-level scattering processes are significantly weaker due to the phonon bottleneck effect in quantum dots.[14,15] Nevertheless, the mechanism and features of Raman scattering in quantum dots have been studied recently,[16,17] showing that Raman spectroscopy is a valuable tool to probe the active optical modes as well as information about the electronic structure in the quantum dots. In this letter, Raman scattering in a self-organized Ge quantum dot superlattice is experimentally investigated.

The sample was grown using a solid source molecular beam epitaxy (MBE) system. A Si(100) wafer with the resistivity of 14–22 Ω cm was cleaned using a standard Shiraki's cleaning method and introduced into the MBE chamber immediately. The protective oxide layer was removed by subsequent heating of the substrate to 930 °C for 15 min. The substrate temperature was maintained at 650 °C during the epitaxial growth. The nominal growth rates were 1 and 0.2 Å/s for Si and Ge, respectively. Boron doping was achieved by thermal evaporation. With this condition, a 200 nm undoped Si buffer layer was first grown, followed by 20 periods of thin heavily boron-doped Ge quantum dot layers sandwiched by two 6 nm undoped Si layers. Figure 1 shows a cross-sectional transmission electron microscopy (TEM) image of the sample. 20 periods of lens-shaped Ge dots are evident, however, vertical correlation[18,19] is not observed in this case, which may be due to the large Si spacer thickness (6 nm). A similar sample without the last Si barrier (with Ge quantum dots grown on the surface) was also examined with atomic force microscopy (AFM), showing a typical base dimension of 420 Å, and a height of 40 Å, which is larger than the data obtained by TEM (37 Å in height). The effect due to the shape of the AFM tip may be a reason.[20] Another reason is the fact that multiple quantum dots are usually flattened in the sandwiched spacer layers.[21] The nonuniformity of the dot size is estimated to be ±10%. The area density of the dots is 1×10^{8} cm^{-2}.

The Raman scattering was performed using a Renishaw Raman Imaging 2000 microscope at room temperature. All spectra were excited by the 514 nm line of an Ar ion laser in the backscattering configuration and recorded by a Si charge-

[a]Electronic mail: jliu@ee.ucla.edu

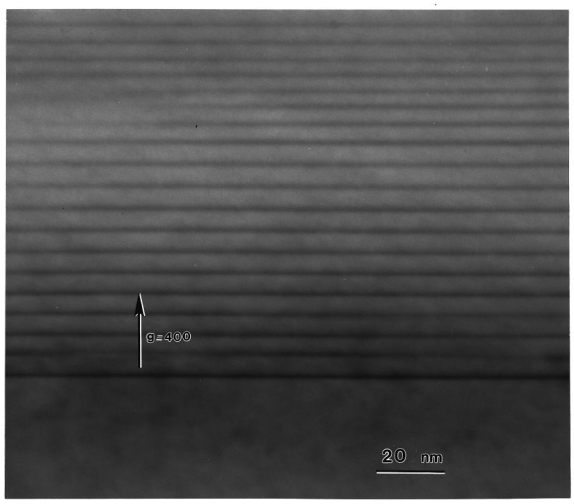

FIG. 1. Cross-sectional TEM image of the self-organized Ge dot superlattice used in this study. The structure consists of 20 periods of Ge dots and 6 nm Si spacers.

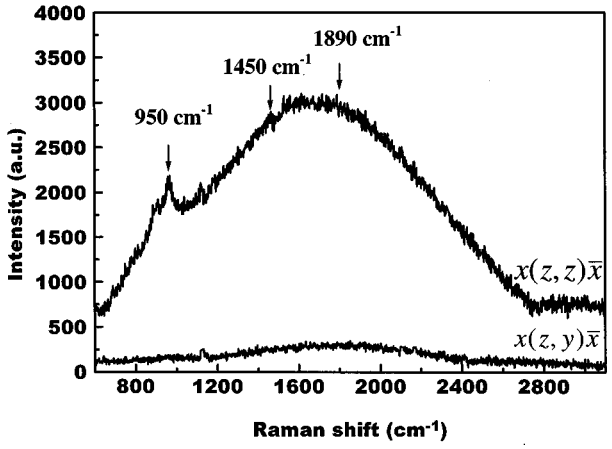

FIG. 3. Polarization dependence of Raman spectra of the sample. The arrows at about 950, 1450, and 1890 cm^{-1} indicate the second Si optical phonon, the third optical phonon, and the inter-sub-level transitions in the Ge dots, respectively.

coupled device (CCD) camera. Figure 2 shows the Raman spectrum of the sample. In this low frequency range, the laser beam is perpendicular to the sample surface and no incident light or scattered light polarization is employed. Besides the strong Si substrate signal at 520 cm^{-1}, Ge–Ge, Si–Ge, and local Si–Si vibrational peaks can be seen at about 301, 403, and 436 cm^{-1}, respectively. The appearance of the Si–Ge and local Si–Si vibrational peaks implies the formation of SiGe alloy in the wetting layers and the existence of strain in Si underneath the dots. In addition, pure Ge is present, which is confirmed by the observed intensity ratio $I(\text{Ge–Ge})/I(\text{Si–Ge})$.[22] Moreover, we conclude that the Ge–Ge peak arises from the Ge dots rather than from the wetting layer. This is argued from the fact that the Ge–Ge peak position of pure, strained Ge (assumed in the wetting layers) should be larger than 306 cm^{-1}.[23,24] The strong phonon confinement in the dots leads to the downward shift of the Ge–Ge peak to 301 cm^{-1} in our sample.

Figure 3 shows the polarization dependent Raman spectra of the sample. In this high frequency range, the incident light is focused on the cleaved edge side of the sample. The polarization of the incident and scattered light is parallel to the growth direction (z) or perpendicular to the growth direction (y). In the polarized spectrum $[x(z,z)\bar{x}]$, two peaks at about 950 and 1450 cm^{-1} are attributed to the second- and third-order Si optical phonons. One peak at about 1890 cm^{-1} with a full-width at half-maximum (FWHM) of 100 meV is related to the inter-sub-levels within the valence band of the Ge dots. Obviously, the considerably large FWHM arises from the size nonuniformity of the quantum dots and the nonparabolicity of the hole bands. We will later show that this peak is strongly related to the first two quantized heavy hole (HH) states in the Ge dots. In the depolarized spectrum $[x(z,y)\bar{x}]$, there are no clear observable phonon peaks in the investigated range because the Si optical phonons are forbidden in principle in this case. The absence of an intersubband transition in the spectrum is due to the fact that the Raman tensor is zero in this configuration according to the selection rules.[25,26]

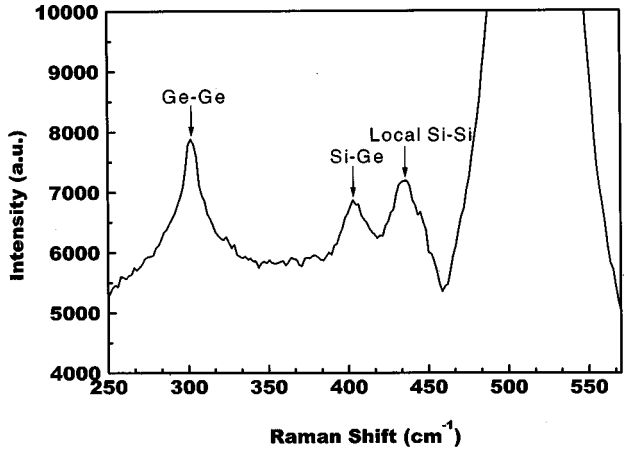

FIG. 2. Typical Raman spectrum of the sample. Ge–Ge, Si–Ge, and local Si–Si optical modes can be found at around 301, 403, and 436 cm^{-1}, respectively.

The inter-sub-level transition at about 1890 cm^{-1} was evaluated by calculating the inter-sub-level energies within the valence band. Details of the calculation process have been described elsewhere.[10] In this simple numerical model, we treated Ge dots as quantum boxes and did not take the valence band mixing, depolarization, and Coulomb interaction into account. Because the lateral dimensions of the present Ge dots (420 Å) are much larger than their heights (37 Å), the quantum confinement effect in the lateral direction can be omitted. Thus, the allowed energies in the dots can be written as

$$E_l = \frac{\pi^2 \hbar^2 l^2}{2m^* L_Z^2}, \quad l = 1,2,3,\ldots, \tag{1}$$

where m^* is the Ge hole effective mass. L_Z is the height of the dots. The calculated results for the present dot sample are illustrated in Fig. 4, indicating that there are two quantized HH states at 91.2 meV (HH1) and 363.2 meV (HH2) in the potential well while the light hole (LH) states and the spin-orbit (SO) split states can only exist near the top of the Si potential barrier or higher. Obviously, the LH and SO states do not contribute to the transition peak observed in the po-

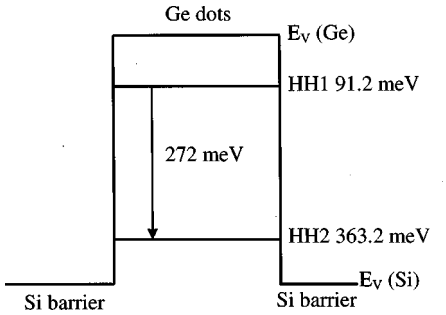

FIG. 4. Schematic representation of the valence band diagram of the sample. The arrow indicates the HH1 to HH2 transition.

larized Raman spectrum. The calculated energy separation between the first two HH states is 272 meV, which is comparable to the measured peak energy of 235.4 meV (1890 cm^{-1}). The difference between the observed and calculated energies may come from the simple model itself as well as depolarization and exciton-like shifts.[27] Thus, we believe this simple calculation reveals the nature of the observed results that the Raman peak at 1890 cm^{-1} arises from the inter-sub-level transition between the first two confined HH states in the Ge quantum dots.

In conclusion, we have reported the Raman scattering form a self-organized Ge dot superlattice. Phonon confinement effect is observed for the embedded Ge dots in Si matrix. An optical transition at 1890 cm^{-1} has been observed in the polarized Raman spectrum, which is attributed to the inter-sub-level transition between the first two confined HH states in the Ge quantum dots. This study provides an impetus for developing improved Si-based midinfrared detectors.

The work was in part supported by the National Science Foundation (DMR-9520893), ARO (DAAG55-98-1-0358), and Low Power MURI (DAAH049610005).

[1] P. M. Petroff and G. Mederios-Riberio, Mater. Res. **21**, 50 (1996).
[2] J.-Y. Marzin, J.-M. Gerand, A. Izrael, D. Barrier, and G. Bastard, Phys. Rev. Lett. **73**, 716 (1994).
[3] H. Sunamara, N. Usami, Y. Shiraki, and S. Fukatsu, Appl. Phys. Lett. **66**, 3024 (1995).
[4] O. G. Schmidt, G. Lange, K. Eberl, O. Kienzle, and F. Ernst, Appl. Phys. Lett. **71**, 2340 (1997).
[5] N. Kirstaedter, N. N. Ledentsov, M. Grundman, D. Bimberg, V. M. Ustinov, S. S. Ruvimov, M. V. Maximov, P. S. Kopev, Zh. I. Alferov, U. Richter, P. Werner, U. Gosele, and J. Heydenreich, Electron. Lett. **30**, 1416 (1994).
[6] H. Drexler, D. Leonard, W. Hansen, J. P. Kotthaus, G. Medeires-Ribeiro, and P. M. Petroff, Phys. Rev. Lett. **73**, 2252 (1994).
[7] J. Phillips, K. Kamath, X. Zhou, N. Chervela, and P. Bhattacharya, Appl. Phys. Lett. **71**, 2079 (1997).
[8] K. W. Berryman, S. A. Lyon, and M. Segev, Appl. Phys. Lett. **70**, 1861 (1997).
[9] A. Sa'ar, J. Appl. Phys. **74**, 5263 (1993).
[10] J. L. Liu, W. G. Wu, A. Balandin, G. Jin, and K. L. Wang, Appl. Phys. Lett. **74**, 185 (1999).
[11] Ch. Zeller, B. Vinter, G. Abstreiter, and K. Ploog, Phys. Rev. B **26**, 2124 (1982).
[12] Y. B. Li, R. A. Stradling, L. Artus, S. J. Webb, R. Cusco, S. J. Chung, and A. G. Norman, Semicond. Sci. Technol. **11**, 1137 (1996).
[13] F. Cereira, A. Pinczuk, and J. C. Bean, Phys. Rev. B **31**, 1202 (1985).
[14] U. Bockelmann and G. Bastard, Phys. Rev. B **42**, 8947 (1990).
[15] H. Benisty, C. M. Sotomayer-Torres, and C. Weisbuch, Phys. Rev. B **44**, 10945 (1991).
[16] E. Menendez, C. Trallero-Giner, and M. Cardona, Phys. Status Solidi B **199**, 81 (1997).
[17] E. Menendez-Proupin, J. L. Pena, and C. Trallero-Giner, Semicond. Sci. Technol. **13**, 871 (1998).
[18] J. Tersoff, C. Teichert, and M. G. Lagally, Phys. Rev. Lett. **76**, 1675 (1996).
[19] P. Schittenhelm, G. Abstreiter, A. Darhuber, G. Bauer, P. Werner, and A. Kosogov, Thin Solid Films **294**, 291 (1997).
[20] K. Sakamoto, H. Matsuhata, M. O. Tanner, D. Wang, and K. L. Wang, Thin Solid Films **321**, 55 (1998).
[21] S. Schierker, O. G. Schmidt, K. Eberl, N. Y. Jin-Phillipp, and F. Phillipp, Appl. Phys. Lett. **72**, 3344 (1998).
[22] E. Molinari and A. Fasolino, Appl. Phys. Lett. **54**, 1220 (1989).
[23] W. J. Brya, Solid State Commun. **12**, 253 (1973).
[24] F. Cerdeira, A. Pinczuk, J. C. Bean, B. Batlogg, and B. A. Wilson, Appl. Phys. Lett. **45**, 1138 (1984).
[25] Y. B. Li, R. A. Stradling, L. Artus, S. J. Webb, R. Cusco, S. J. Chung, and A. G. Norman, Semicond. Sci. Technol. **11**, 1137 (1996).
[26] M. Bendayan, R. Beserman, and K. Dettmer, J. Appl. Phys. **81**, 7956 (1997).
[27] K. L. Wang and R. P. G. Karunasiri, *Semiconductor Quantum Wells and Superlattices for Long-Wavelength Infrared Detectors*, edited by M. O. Manasreh (Artech House, Boston, 1993), p. 139.